Regular Article

Structure–Activity Relationship Study of N^6-Benzoyladenine-Type BRD4 Inhibitors and Their Effects on Cell Differentiation and TNF-α Production

Seika Amemiya, Takao Yamaguchi, Taki Sakai, Yuichi Hashimoto, and Tomomi Noguchi-Yachide*

Institute of Molecular & Cellular Biosciences, The University of Tokyo; 1–1–1 Yayoi, Bunkyo-ku, Tokyo 113–0032, Japan.

Received May 16, 2016; accepted June 13, 2016

Bromodomains are epigenetic 'readers' of histone acetylation. The first potent bromodomain and extra-terminal domain (BET) inhibitors, (+)-JQ1 and I-BET762 (also known as GSK525762), were reported in 2010. Some BET inhibitors are already under clinical trial for the treatment of cancers, but so far, only a few chemical scaffolds are available. We have reported potent N^6-benzoyladenine-based inhibitors of BRD4, a BET family member that serves as a key mediator of transcriptional elongation. Here we present an analysis of the structure–activity relationships of these inhibitors. Among the compounds examined, 20, 28 and 29 enhanced all-*trans* retinoic acid (ATRA)-induced HL-60 cell differentiation and inhibited tumor necrosis factor (TNF)-α production by THP-1 cells.

Key words bromodomain; bromodomain and extra-terminal domain (BET); BRD4; cell differentiation; tumor necrosis factor (TNF)-α

Epigenetic therapy is attracting increasing interest for the treatment of various diseases, including cancers and chronic inflammatory disorders. In particular, small-molecular modulators of epigenetic protein–protein interactions (PPI) are expected to be promising candidates. Indeed, there have been many synthetic studies on inhibitors of histone deacetylase (HDAC), which is an epigenetic 'eraser' involved in regulation of histone acetylation. Among these inhibitors, Vorinostat (suberoylanilide hydroxamic acid; SAHA) has been approved for the treatment of cancers by the U.S. Food and Drug Administration (FDA). Since the first potent bromodomain and extra-terminal domain (BET) inhibitors, (+)-JQ1[1] and I-BET762 (also known as GSK525762),[2] were reported in 2010, small-molecular inhibitors of epigenetic 'readers' of histone acetylation have also been attracting attention.[3] In fact, some BET inhibitors, such as I-BET762, OTX-015, CPI-0610 and RVX208 (Fig. 1), are already in clinical trials for treatment of cancers and cardiovascular diseases.

More than 40 diverse proteins, including BET family proteins and histone acetyltransferases (HATs), contain bromodomains as structural motifs.[4] The human BET family has four members, *i.e.*, BRD2, BRD3, BRD4 and BRDT. They each have tandem amino-terminal bromodomains, which recognize N^{ε}-acetylated lysine residues (Kac) in histones, typically histones H3 and H4.[4,5] Although the detailed functions and precise functional differences among the human four BRD's are still unclear, BRD4 is the most extensively studied, and is one of the key mediators of transcriptional elongation. The bromodomains of BRD4 recruit positive transcriptional elongation factor b (P-TEFb), leading to phosphorylation of RNA polymerase II and transcriptional elongation.[6,7] P-TEFb has been reported to act as a transcriptional activator of c-*myc*, which is a key regulator of cellular processes, including cell proliferation, differentiation and growth, in cancers.[8] Therefore, it is not surprising that BET inhibitors down-regulate MYC and MYC-dependent target genes.[9] Furthermore, down-regulation of MYC in acute myeloid leukaemia (AML) cells by BRD4 induces cell differentiation.[10]

BRD4 also binds to Kac of the RelA subunit of nuclear factor kappa B (NF-κB) transcriptional complex, thereby activating transcription of NF-κB. BRD4-RelA interaction leads to regulation of NF-κB-mediated inflammatory genes, including interleukin (IL)-6 and tumor necrosis factor (TNF)-α.[11] TNF-α is one of the proinflammatory cytokines mediating immune regulation, including modulation of diverse signaling pathways for cell differentiation, proliferation and death.[12,13] TNF-α also has been suggested to be an endogenous tumor promoter.[14,15] Thus, TNF-α plays an important pathophysiological role in not only inflammatory disorders, but also cancers. Hyperacetylated RelA is also involved in Stat3-mediated sustained NF-κB activation in lung cancer.[16]

Therefore, BRD4 is considered to be a promising therapeutic target for treatment of cancers such as AML and NF-κB-driven lung cancer.[17] In addition, there is great interest in developing small-molecular BRD4 inhibitors since only a limited number of template structures as Kac binding motifs have been reported (Fig. 1). From these perspectives, we previously screened our "multi-template" library derived from thalidomide[18] for BRD4-inhibiting activity, and identified N^6-benzoyladenine as a new chemical scaffold for development of BRD4 inhibitors.[19] After our discovery of N^6-benzoyladenine as a BRD4 inhibitor, the related bromodomain inhibitors with 2-amine-9*H*-purine moiety have been reported to form hydrogen bonds with the conserved Asn (N140) in the Kac-binding pocket of BRD4 through purine nitrogens.[20]

In the present report, we discuss the structure–activity relationships (SAR) of BRD4 inhibitors containing the N^6-benzoyladenine moiety. We also evaluated the biological activities of selected compounds, and found that they exhibit all-*trans* retinoic acid (ATRA)-induced HL-60 cell differen-

* To whom correspondence should be addressed. e-mail: noguchi@iam.u-tokyo.ac.jp

Table 1. BRD4-Inhibitory Activity of N^6-(2-Substituted benzoyl)adenines

	Compound	R	IC_{50} (μM)	Compound	R	IC_{50} (μM) or ( ): inhibitory rate at 100 μM
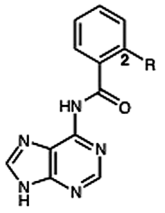	(+)-JQ1	—	0.20			
	1	H	170	**7**	SMe	(49%)
	2	NMe_2	19	**8**	OH	83
	3	OBn	81	**9**	Br	(17%)
	4	OPh	36	**10**	Me	(13%)
	5	$O(CH_2)_4CH_3$	6.9	**11**	NO_2	N.A.
	6	OMe	49	**12**	CF_3	N.A.

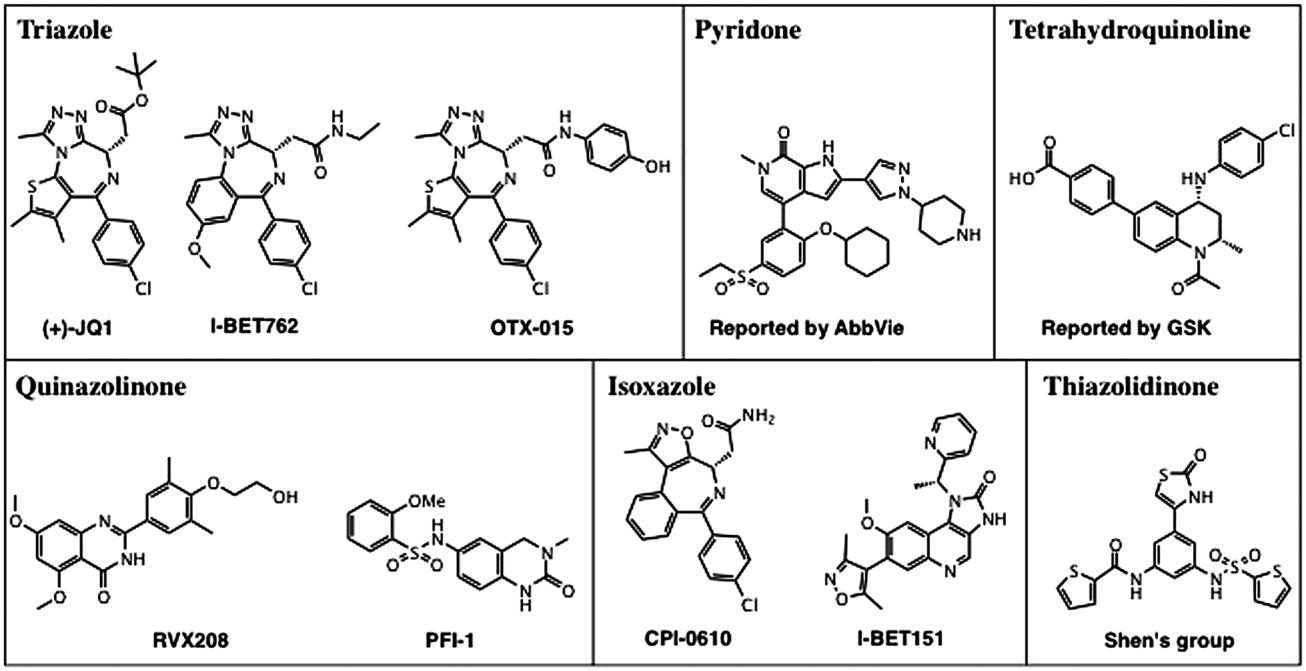

Fig. 1. Structures of Reported BET Inhibitors

tiation-enhancing activity and TNF-α production-inhibitory activity. These results support the view that BRD4 inhibitors containing N^6-benzoyladenine moiety might be useful for cancer therapy.

Results and Discussion

Structure–Activity Relationships (SAR) In order to elucidate the SAR of N^6-benzoyladenine as a BRD4 inhibitor,[19] we first investigated substituent effects at the 2-position of the benzoyl group. The compounds were prepared by a condensation of adenine and substituted benzoic acid (Chart 1). Generally, this condensation gave multiple products probably because adenine has several nucleophilic nitrogen atoms (N^1, N^3, N^6, N^7 and N^9); thus we separated the mixture and obtained N^6-benzoyladenines in *ca.* 10% yields. The BRD4-inhibitory activities of tested compounds were evaluated by means of LANCE time-resolved fluorescence resonance energy transfer (TR-FRET) assay using a Cayman BRD4 bromodomain 1 TR-FRET assay kit. The activities of N^6-(2-substituted benzoyl)-adenines are summarized in Table 1. The BRD4-inhibitory activity of the compounds decreased in the following order: $O(CH_2)_4CH_3$ (**5**)>NMe_2 (**2**)>OPh (**4**)>OMe (**6**)>OBn (**3**)>OH (**8**)>H (**1**)>SMe (**7**)>Br (**9**)>Me (**10**)>NO_2 (**11**)=CF_3 (**12**). As compared to N^6-benzoyladenine (**1**), compounds **2**–**6** and **8** showed more potent activities, and compounds **7** and **9**–**12** showed weaker activities. These results imply that introduction of a possible hydrogen bond acceptor at the 2-position of the benzoyl group and/or a substituent that enhances the hydrogen bond-accepting character of the carbonyl oxygen in the benzoyl moiety would be favorable for potent BRD4-inhibitory activity. Such hydrogen bond(s) can plausibly exist between our N^6-benzoyladenine-type inhibitors and the Kac binding pocket of BRD4.

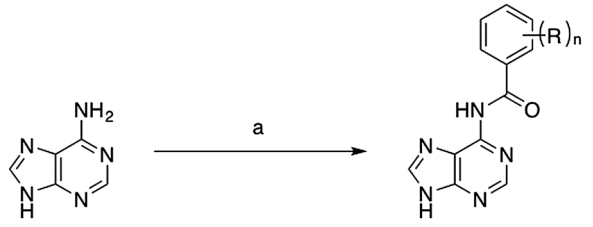

Reagents and conditions: (a) Substituted benzoic acid, EDCI·HCl, DMA, 100–130°C.

Chart 1. General Synthesis of N^6-Benzoyladenine Derivatives

Next, we examined the positional effect of the substituent on the benzoyl moiety. Although 2-substituted compounds **4**–**6** (Table 1) were more potent inhibitors than N^6-benzoyl-

adenine (**1**), the corresponding 3- or 4-substituted compounds (**13**, **15**, **17**, **18**) showed weaker activity, and compounds **14** and **16** were inactive (Table 2). These results indicate that *ortho*-substitution is preferable to *meta*/*para*-substitution for potent BRD4-inhibitory activity.

We then investigated the effects of multiple substituents (Table 3). Among di-substituted derivatives, N^6-[3,5-bis(dimethylamino)benzoyl]adenine (**20**) is slightly more potent than the mono-dimethylamino derivative (**2**), while N^6-(2,5-dimethoxybenzoyl)adenine (**23**) and N^6-(3,4-dimethoxybenzoyl)adenine (**25**) are more potent than the mono-methoxy derivative (**6**). These results prompted us to prepare trimethoxy derivatives (**27**–**29**), and as we had hoped, both N^6-(2,4,5-trimethoxybenzoyl)adenine (**28**) and N^6-(3,4,5-trimethoxybenzoyl)adenine (**29**) showed very potent BRD4-inhibitory activities with IC_{50} values of 3.9 and 6.9 μM, respectively. N^6-(2,4,5-Trimethoxybenzoyl)adenine (**28**) is the most potent BRD4 inhibitor among the N^6-benzoyladenine derivatives examined.

Effect on HL-60 Cell Differentiation Inhibition of BRD4 suppresses MYC expression, leading to terminal myeloid differentiation and elimination of leukemia stem cells.[21] In addition, (+)-JQ1, a BRD4 inhibitor, has a broad-spectrum activity against diverse human leukemia cell lines, including THP-1 (human monocytic leukemia cell line), HL-60 (human promyelocytic leukemia cells) and NB4 (human bone marrow acute promyelocytic leukemia cell line).[21] Therefore, BRD4 is a promising therapeutic target to treat leukemia, especially AML.[10] These reports prompted us to examine the effect of our compounds on ATRA-induced differentiation of HL-60 cells. We selected ATRA because it is an endogenous active metabolite of vitamin A that is commonly present in normal human serum. In addition, ATRA has been established to induce differentiation of HL-60 cells to mature granulocytes, and is in clinical use for treatment of acute promyelocytic leukemia (APL). The enhancing activity of test compounds on ATRA-induced HL-60 cell differentiation was measured as described in Experimental, and results are presented as %-values of nitro blue tetrazolium (NBT)-positive cells (an established measure of differentiated HL-60 cells).

As expected, (+)-JQ1 and N^6-benzoyladenine derivatives **20**, **28** and **29**, all of which possess BRD4-inhibitory activity (Table 3), showed an enhancing effect on ATRA-induced HL-60 cell differentiation (Table 4). On the other hand, compound **12**, which is inactive toward BRD4, did not show cell differentiation-enhancing activity. The population of NBT-positive cells in HL-60 cells exposed to 0.6 nM ATRA in the presence of compounds **20**, **28** and **29** exceeded that of HL-60 cells exposed to 0.6 nM ATRA alone (13% NBT-positive cells in Fig. 2A). The cell differentiation-enhancing effects elicited by **20**, **28** and **29** were dose-dependent (Fig. 2A), and decreased in the following order: 2,4,5-$(OMe)_3$ (**28**)>3,4,5-$(OMe)_3$ (**29**)>3,5-$(OMe)_2$ (**20**). This is the same as the decreasing order of BRD4-inhibitory activity of these compounds (Table 3).

Cell differentiation was morphologically evaluated by microscopy after Wright–Giemsa staining. As shown in Fig. 2B,

Table 2. Effect of Substitution Site in the Benzoyl Moiety on BRD4-Inhibitory Activity

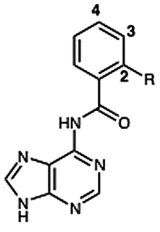

Compound	R	IC_{50} (μM) or ( ): inhibitory rate at 100 μM
(+)-JQ1	—	0.20
1	H	170
4	2-OPh	36
13	3-OPh	(40%)
14	4-OPh	N.A.
5	2-$O(CH_2)_4CH_3$	6.9
15	3-$O(CH_2)_4CH_3$	(27%)
16	4-$O(CH_2)_4CH_3$	N.A.
6	2-OMe	49
17	3-OMe	(43%)
18	4-OMe	*ca.* 100

Table 4. EC_{50} Values for ATRA-Induced HL-60 Cell Differentiation-Enhancing Activity

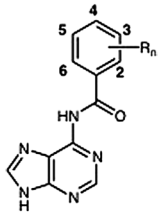

Compound	R	EC_{50} (μM)
(+)-JQ1	—	0.050
12	2-CF_3	N.A.
20	3,5-$(NMe_2)_2$	7.4
28	2,4,5-$(OMe)_3$	1.9
29	3,4,5-$(OMe)_3$	6.9

Table 3. Effect of Multiple Substituents in the Benzoyl Moiety on BRD4-Inhibitory Activity

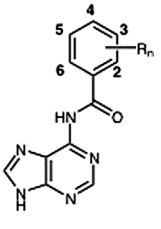

Compound	R	IC_{50} (μM) or ( ): inhibitory rate at 100 μM	Compound	R	IC_{50} (μM) or ( ): inhibitory rate at 100 μM
(+)-JQ1	—	0.20	**22**	2,4-$(OMe)_2$	N.A.
2	2-NMe_2	19	**23**	2,5-$(OMe)_2$	33
19	3,4-$(NMe_2)_2$	49	**24**	2,6-$(OMe)_2$	(7%)
20	3,5-$(NMe_2)_2$	15	**25**	3,4-$(OMe)_2$	24
6	2-OMe	49	**26**	3,5-$(OMe)_2$	55
17	3-OMe	(43%)	**27**	2,3,4-$(OMe)_3$	36
18	4-OMe	*ca.* 100	**28**	2,4,5-$(OMe)_3$	3.9
21	2,3-$(OMe)_2$	95	**29**	3,4,5-$(OMe)_3$	6.9

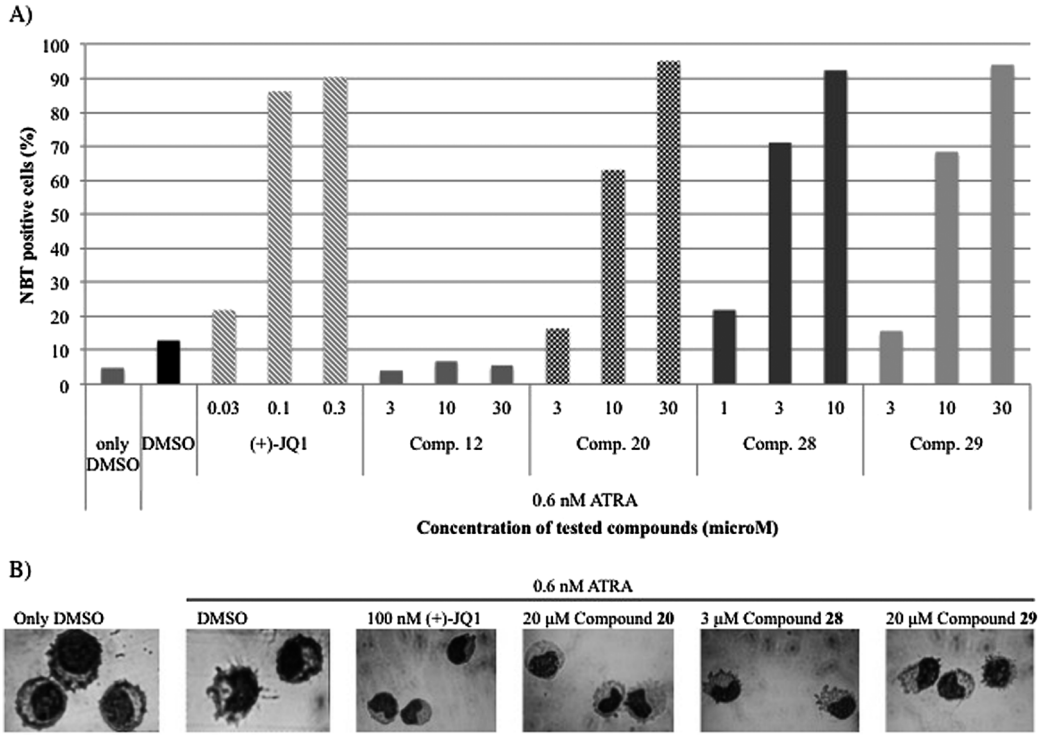

Fig. 2. ATRA-Induced HL-60 Cell Differentiation-Enhancing Activity (A) and Results of Wright–Giemsa Staining (B)

Panel A: percentage of NBT-positive cells treated with tested compounds or DMSO in the presence or absence of 0.6 nM ATRA. Panel B: typical morphology of HL-60 cells treated with the compound(s) indicated.

HL-60 cells treated by (+)-JQ1 and compounds **20**, **28** and **29** in the presence of ATRA exhibit the following change: smaller nuclear size, decreased nuclear/cytoplasmic ratio and banded nuclei. These treatments resulted in differentiation to mature granulocytes. ATRA is a retinoic acid receptor (RAR) agonist. However, compounds **20**, **28** and **29** did not activate RAR as far as investigated by a reporter gene assay method. Thus, one possible mechanism of the observed differentiation-enhancing activity is *via* inhibition of BRD4. A detailed mechanistic analysis is in progress. These results suggest that cancer therapy with BRD4 inhibitors might result in effective induction of leukemia cell differentiation, because normal serum contains nanomolar-order concentration of ATRA, at which concentration compounds **20**, **28** and **29** would cause enhancement of cell differentiation. It is also possible that coadministration of BRD4 inhibitors in ATRA differentiation-inducing therapy would make it possible to lower the required dose of ATRA.

TNF-*α* Production-Inhibitory Activity The bromodomains of BRD4 recruit P-TEFb, thereby regulating expression of genes related to inflammation and cancer, including *Tnf* and c-*myc*. Thus, we next investigated the effect of our N^6-benzoyladenine-type BRD4 inhibitors on TNF-*α* production by means of a previously reported enzyme-linked immunosorbent assay (ELISA) method, using a human monocytic leukemia cell line, THP-1.[22,23] THP-1 cells under normal cell culture conditions do not produce TNF-*α*, but TNF-*α* production is induced by treatment with 12-*O*-tetradecanoylphorbol 13-acetate (TPA).

As we had expected, compounds **20**, **28** and **29**, all of which exhibit BRD4-inhibitory activity (Table 3), inhibited TPA-induced TNF-*α* production by THP-1 cells (Table 5). On the other hand, compound **12**, which did not possess BRD4-inhibitory activity, was inactive. Compound **28** showed the most potent activity among the N^6-benzoyladenine-type BRD4 inhibitors, with an IC_{50} value of 1.6 μM; this compound was also the most potent BRD4 inhibitor (Table 3). These results suggest that N^6-benzoyladenine-type BRD4 inhibitors might be candidate agents for cancer chemotherapy.

Table 5. TNF-*α* Production-Inhibitory Activity

Compound	R	IC_{50} (μM)
(+)-JQ1	—	0.073
12	2-CF_3	N.A.
20	3,5-$(NMe_2)_2$	6.5
28	2,4,5-$(OMe)_3$	1.6
29	3,4,5-$(OMe)_3$	6.5

Conclusions and Prospects We examined the SAR of N^6-benzoyladenine derivatives for BRD4-inhibitory activity, and identified potent BRD4 inhibitors **28** and **29**. We also found that BRD4 inhibitors **20**, **28** and **29** enhance ATRA-induced HL-60 cell differentiation and inhibit TPA-induced TNF-*α* production by THP-1 cells. Further studies of the mechanisms of these activities and evaluation of anti-cancer activity are in progress. The results so far suggest that N^6-benzoyladenine-type BRD4 inhibitors are promising candidates for cancer chemotherapy.

Experimental

General Chemistry All chemical reagents and solvents were purchased from Sigma-Aldrich Co., LLC, Kanto

Chemical Co., Inc. (Japan), Tokyo Chemical Industry Co., Ltd. (Japan) and Wako Pure Chemical Industries, Ltd. (Japan), and used without further purification. Moisture-sensitive reactions were performed under an atmosphere of argon, unless otherwise noted, and monitored by thin-layer chromatography (TLC, Merck silica gel 60 F254 plates). Bands were visualized using UV light or by application of appropriate reagents followed by heating. Flash chromatography was carried out with silica gel (Silica gel 60N, 40–50 μm particle size) purchased from Kanto Chemical Co., Inc. NMR spectra were recorded on a JEOL JNM-GX500 (500 MHz) spectrometer, operating at 500 MHz for ^{1}H-NMR and at 125 MHz for ^{13}C-NMR. Proton and carbon chemical shifts are expressed in δ values (ppm) relative to internal tetramethylsilane (0.00 ppm) or residual $CHCl_3$ (7.26 ppm) for ^{1}H-NMR, and internal tetramethylsilane (0.00 ppm) or $CDCl_3$ (77.16 ppm) for ^{13}C-NMR. Data are reported as follows: chemical shift, multiplicity (s, singlet; d, doublet; t, triplet; q, quartet; m, multiplet; br, broad), coupling constants (Hz), integration. High-resolution (HR)-MS were recorded using a Bruker micrOTOF II mass spectrometer.

General Synthetic Procedure for N^6-Benzoyladenine Derivatives Benzoic acid (1.0 eq) and 1-ethyl-3-(3-dimethylaminopropyl)carbodiimide hydrochloride (1.2 eq) were added to a suspension of adenine (1.0 eq) in anhydrous *N*-dimethylacetamide (DMA), and the mixture was stirred at 100–130°C. After completion of the reaction, the solvent was removed under reduced pressure. The residue was purified by silica gel column chromatography (MeOH–$CHCl_3$) and by washing with AcOEt and/or CH_2Cl_2–hexane (1 : 1 or 1 : 0) to afford the product.

N^6-(2-Benzyloxybenzoyl)adenine (**3**)

White solid (0.3%): mp 131.0–132.0°C; ^{1}H-NMR (500 MHz, DMSO-d_6) δ: 5.33 (s, 2H), 7.14 (dd, J=6.9, 8.0 Hz, 1H), 7.25–7.35 (m, 4H), 7.54 (d, J=6.9 Hz, 2H), 7.59 (dd, J=7.5, 8.6 Hz, 1H), 7.88 (d, J=7.4 Hz, 1H), 8.55 (s, 1H), 8.66 (s, 1H), 11.18 (brs, 1H); electrospray ionization (ESI)-time-of-flight (TOF)-HR-MS $(M+Na)^+$ Calcd for $C_{19}H_{15}N_5O_2$ 368.1118. Found 368.1113.

N^6-(2-Phenoxybenzoyl)adenine (**4**)

White solid (3%): mp 210.0–210.5°C; ^{1}H-NMR (500 MHz, DMSO-d_6) δ: 6.90 (d, J=8.0 Hz, 1H), 7.10 (d, J=8.0 Hz, 2H), 7.14 (dd, J=7.5, 7.5 Hz, 1H), 7.26 (dd, J=7.4, 7.5 Hz, 1H), 7.37 (dd, J=7.5, 8.0 Hz, 2H), 7.53 (dd, J=7.5, 7.5 Hz, 1H), 7.83 (d, J=6.9 Hz, 1H), 8.62 (s, 1H), 8.66 (s, 1H), 11.42 (brs, 1H); ESI-TOF-HR-MS $(M+Na)^+$ Calcd for $C_{18}H_{13}N_5O_2$ 354.0961. Found 354.0954.

N^6-(2-Pentyloxybenzoyl)adenine (**5**)

White solid (10%): mp 176.5–177.0°C; ^{1}H-NMR (500 MHz, DMSO-d_6) δ: 0.80 (t, J=7.4 Hz, 3H), 1.28–1.35 (m, 2H), 1.43–1.49 (m, 2H), 1.82–1.88 (m, 2H), 4.22 (t, J=6.3 Hz, 2H), 7.14 (dd, J=6.9, 7.5 Hz, 1H), 7.27 (d, J=8.6 Hz, 1H), 7.61 (dd, J=7.7, 7.8 Hz, 1H), 7.98 (d, J=7.5 Hz, 1H), 8.61 (s, 1H), 8.67 (s, 1H), 11.13 (brs, 1H); ESI-TOF-HR-MS $(M+Na)^+$ Calcd for $C_{17}H_{19}N_5O_2$ 348.1431. Found 348.1420.

N^6-(2-Nitrobenzoyl)adenine (**11**)

Yellow solid (3%): mp 236.0–237.0°C; ^{1}H-NMR (500 MHz, DMSO-d_6) δ: 7.77–7.89 (m, 3H), 8.18 (d, J=8.0 Hz, 1H), 8.47 (s, 1H), 8.65 (s, 1H), 11.93 (s, 1H), 12.27 (s, 1H); ESI-TOF-HR-MS $(M+Na)^+$ Calcd for $C_{12}H_8N_6O_3$ 307.0550. Found 307.0546.

N^6-(2-Trifluorobenzoyl)adenine (**12**)

White solid (4%): mp 232.5–233.0°C; ^{1}H-NMR (500 MHz, DMSO-d_6) δ: 7.71–7.74 (m, 3H), 7.85 (d, J=8.0 Hz, 1H), 8.47 (s, 1H), 8.65 (s, 1H), 11.81 (s, 1H), 12.28 (s, 1H); ESI-TOF-HR-MS $(M+Na)^+$ Calcd for $C_{13}H_8F_3N_5O$ 303.0573. Found 330.0576.

N^6-(3-Phenoxybenzoyl)adenine (**13**)

White solid (17%): mp 201.0–202.0°C; ^{1}H-NMR (500 MHz, DMSO-d_6) δ: 7.06 (d, J=8.0 Hz, 2H), 7.16 (dd, J=7.5, 7.5 Hz, 1H), 7.30 (d, J=8.0 Hz, 1H), 7.40 (dd, J=7.4, 8.6 Hz, 2H), 7.55 (dd, J=8.0, 8.1 Hz, 1H), 7.65 (s, 1H), 7.88 (d, J=8.0 Hz, 1H), 8.45 (s, 1H), 8.69 (s, 1H), 11.57 (brs, 1H), 12.34 (brs, 1H); ESI-TOF-HR-MS $(M+Na)^+$ Calcd for $C_{18}H_{13}N_5O_2$ 354.0961. Found 354.0963.

N^6-(4-Phenoxybenzoyl)adenine (**14**)

White solid (21%): mp 246.5–247.0°C; ^{1}H-NMR (500 MHz, DMSO-d_6) δ: 7.07 (d, J=6.9 Hz, 2H), 7.12 (d, J=8.6 Hz, 2H), 7.23 (dd, J=7.5, 7.5 Hz, 1H), 7.45 (dd, J=7.5, 8.6 Hz, 2H), 8.13 (d, J=9.2 Hz, 2H), 8.45 (s, 1H), 8.68 (s, 1H), 11.46 (brs, 1H), 12.33 (brs, 1H); ESI-TOF-HR-MS $(M+Na)^+$ Calcd for $C_{18}H_{13}N_5O_2$ 354.0961. Found 354.0961.

N^6-(3-Pentyloxybenzoyl)adenine (**15**)

White solid (14%): mp 156.0–156.5°C; ^{1}H-NMR (500 MHz, DMSO-d_6) δ: 0.87 (t, J=7.5 Hz, 3H), 1.29–1.42 (m, 4H), 1.69–1.75 (m, 2H), 4.04 (t, J=6.9 Hz, 2H), 7.17 (d, J=8.3 Hz, 1H), 7.43 (dd, J=8.0, 8.0 Hz, 1H), 7.64 (brs, 2H), 8.47 (s, 1H), 8.70 (s, 1H), 11.50 (s, 1H), 12.34 (s, 1H); ESI-TOF-HR-MS $(M+Na)^+$ Calcd for $C_{17}H_{19}N_5O_2$ 348.1431. Found 348.1425.

N^6-(4-Pentyloxybenzoyl)adenine (**16**)

White solid (26%): mp 214.5–215.0°C; ^{1}H-NMR (500 MHz, DMSO-d_6) δ: 0.88 (t, J=7.5 Hz, 3H), 1.32–1.39 (m, 4H), 1.69–1.75 (m, 2H), 4.05 (t, J=6.9 Hz, 2H), 7.05 (d, J=8.6 Hz, 2H), 8.08 (d, J=8.6 Hz, 2H), 8.44 (s, 1H), 8.68 (s, 1H), 11.32 (s, 1H); ESI-TOF-HR-MS $(M+Na)^+$ Calcd for $C_{17}H_{19}N_5O_2$ 348.1431. Found 348.1419.

N^6-[3,4-Bis(dimethylamino)benzoyl]adenine (**19**)

Yellow solid (3%): mp 153.0–154.0°C; ^{1}H-NMR (500 MHz, DMSO-d_6) δ: 2.79 (s, 6H), 2.88 (s, 6H), 7.04 (d, J=8.1 Hz, 1H), 7.75–7.79 (m, 2H), 8.50 (s, 1H), 8.70 (s, 1H); ESI-TOF-HR-MS $(M+Na)^+$ Calcd for $C_{16}H_{19}N_7O$ 348.1543. Found 348.1531.

N^6-[3,5-Bis(dimethylamino)benzoyl]adenine (**20**)

Yellow solid (4%): mp 113.5–114.5°C; ^{1}H-NMR (500 MHz, DMSO-d_6) δ: 2.97 (s, 12H), 6.39 (s, 1H), 6.80 (s, 2H), 8.29 (s, 1H), 8.65 (s, 1H); ESI-TOF-HR-MS $(M+Na)^+$ Calcd for $C_{16}H_{19}N_7O$ 348.1543. Found 348.1551.

N^6-(2,3,4-Trimethoxybenzoyl)adenine (**27**)

Pale yellow solid (1%): mp 127.0–128.0°C; ^{1}H-NMR (500 MHz, $CDCl_3$) δ: 3.87 (s, 3H), 3.97 (s, 3H), 4.20 (s, 3H), 6.88 (d, J=8.6 Hz, 1H), 7.90 (d, J=8.6 Hz, 1H), 9.17 (s, 1H), 9.47 (s, 1H), 11.74 (brs, 1H); ESI-TOF-HR-MS $(M+Na)^+$ Calcd for $C_{15}H_{15}N_5O_4$ 352.1016. Found 352.1019.

N^6-(3,4,5-Trimethoxybenzoyl)adenine (**29**)

White solid (17%): mp 149.5–150.5°C; ^{1}H-NMR (500 MHz, DMSO-d_6) δ: 3.73 (s, 3H), 3.85 (s, 6H), 7.48 (s, 2H), 8.45 (s, 1H), 8.71 (s, 1H), 11.52 (s, 1H), 12.35 (s, 1H); ESI-TOF-HR-MS $(M+Na)^+$ Calcd for $C_{15}H_{15}N_5O_4$ 352.1016. Found 352.1018.

BRD4 Bromodomain 1 TR-FRET Assay BRD4-inhibitory activities of tested compounds were measured as previously described[19] by means of europium-based LANCE TR-FRET assay using a BRD4 bromodomain 1 TR-FRET assay kit (Item No. 600520, Cayman). (+)-JQ1 (Item No. 11187, Cayman) was used as a positive control. Plates were read in the time-resolved format by exciting the tested com-

pounds at 320 nm and reading emissions at 615 and 665 nm, using a 100 μs delay and a 400 μs read window in Envision (PerkinElmer, Inc.). Data analysis was performed using the TR-FRET ratio (665 nm emission/615 nm emission).

Cell Culture HL-60 cells and THP-1 cells were cultured in RPMI 1640 supplemented with 10% fetal bovine serum (FBS) and penicillin–streptomycin at 37°C in a humidified incubator (5% CO_2 in air).

Assay of Cell Differentiation-Inducing Activity HL-60 cells were maintained and their differentiation was evaluated as previously described.[24–26] Briefly, HL-60 cells (1.0×10^5 cells/mL) were incubated in RPMI 1640 medium supplemented with 10% (v/v) FBS in 24-well plates and treated with a test compound or DMSO. After incubation for 1 h, cells were treated with 0.6 nM ATRA or DMSO and incubated at 37°C under a 5% CO_2 atmosphere for 3 d. Then the treated HL-60 cells were mixed with phosphate-buffered saline (PBS) containing 0.2% (w/v) NBT and 20 nM TPA in a 1 : 1 (v/v) ratio and incubated at 37°C under a 5% CO_2 atmosphere for 30 min. NBT positivity was measured by counting 200–400 cells. Cell differentiation was also confirmed morphologically by microscopy after Wright–Giemsa staining, using ATRA as a positive control compound, which has been established to induce differentiation of HL-60 cells to mature granulocytes. The results were basically reproducible and a typical set of data (mean values of duplicate determinations) obtained at the same time is presented in Table 4.

Assay of TNF-α Production-Inhibiting Activity THP-1 cells were maintained and measurement of TNF-α was performed as previously described.[22,23] Briefly, exponentially growing THP-1 cells (1.0×10^6 cells/mL) were incubated in RPMI1640 medium supplemented with 15% (v/v) FBS in the presence or absence of a test compound with or without 20 nM TPA at 37°C under a 5% CO_2 atmosphere for 18 h in 24-well multi-plates. The cells were collected by centrifugation (1500 rpm×10 min), and the amount of TNF-α in the supernatant was measured by the use of TNF-α ELISA kit, Human (Thermo Fisher Scientific, EH3TNFA) according to the supplier's protocol. The concentration of TNF-α produced by THP-1 cells treated with 20 nM TPA alone was approximately 150 pg/mL under these experimental conditions. The assay was performed at least three times and the results were basically reproducible. A typical set of data (mean values of duplicate determinations) obtained at the same time is presented in Table 5.

Acknowledgments The work described in this paper was partially supported by Grants-in-Aid for Scientific Research from the Ministry of Education, Culture, Sports, Science and Technology of Japan, and the Japan Society for Promotion of Science, and Platform for Drug Discovery, Informatics, and Structural Life Science.

Conflict of Interest The authors declare no conflict of interest.

References

1) Filippakopoulos P., Qi J., Picaud S., Shen Y., Smith W. B., Fedorov O., Morse E. M., Keates T., Hickman T. T., Felletar I., Philpott M., Munro S., McKeown M. R., Wang Y., Christie A. L., West N., Cameron M. J., Schwartz B., Heightman T. D., La Thangue N., French C. A., Wiest O., Kung A. L., Knapp S., Bradner J. E., *Nature* (London), **468**, 1067–1073 (2010).
2) Nicodeme E., Jeffrey K. L., Schaefer U., Beinke S., Dewell S., Chung C. W., Chandwani R., Marazzi I., Wilson P., Coste H., White J., Kirilovsky J., Rice C. M., Lora J. M., Prinjha R. K., Lee K., Tarakhovsky A., *Nature* (London), **468**, 1119–1123 (2010).
3) Romero F. A., Taylor A. M., Crawford T. D., Tsui V., Côté A., Magnuson S., *J. Med. Chem.*, **59**, 1271–1298 (2016).
4) Filippakopoulos P., Picaud S., Mangos M., Keates T., Lambert J. P., Barsyte-Lovejoy D., Felletar I., Volkmer R., Müller S., Pawson T., Gingras A. C., Arrowsmith C. H., Knapp S., *Cell*, **149**, 214–231 (2012).
5) Dey A., Chitsaz F., Abbasi A., Misteli T., Ozato K., *Proc. Natl. Acad. Sci. U.S.A.*, **100**, 8758–8763 (2003).
6) Jang M. K., Mochizuki K., Zhou M., Jeong H. S., Brady J. N., Ozato K., *Mol. Cell*, **19**, 523–534 (2005).
7) Yang Z., Yik J. H., Chen R., He N., Jang M. K., Ozato K., Zhou Q., *Mol. Cell*, **19**, 535–545 (2005).
8) Rahl P. B., Lin C. Y., Seila A. C., Flynn R. A., McCuine S., Burge C. B., Sharp P. A., Young R. A., *Cell*, **141**, 432–445 (2010).
9) Delmore J. E., Issa G. C., Lemieux M. E., Rahl P. B., Shi J., Jacobs H. M., Kastritis E., Gilpatrick T., Paranal R. M., Qi J., Chesi M., Schinzel A. C., McKeown M. R., Heffernan T. P., Vakoc C. R., Bergsagel P. L., Ghobrial I. M., Richardson P. G., Young R. A., Hahn W. C., Anderson K. C., Kung A. L., Bradner J. E., Mitsiades C. S., *Cell*, **146**, 904–917 (2011).
10) Zuber J., Shi J., Wang E., Rappaport A. R., Herrmann H., Sison E. A., Magoon D., Qi J., Blatt K., Wunderlich M., Taylor M. J., Johns C., Chicas A., Mulloy J. C., Kogan S. C., Brown P., Valent P., Bradner J. E., Lowe S. W., Vakoc C. R., *Nature* (London), **478**, 524–528 (2011).
11) Huang B., Yang X. D., Zhou M. M., Ozato K., Chen L. F., *Mol. Cell. Biol.*, **29**, 1375–1387 (2009).
12) Wallach D., *Cytokine Growth Factor Rev.*, **7**, 211–221 (1996).
13) Pasparakis M., Alexopoulou L., Douni E., Kollias G., *Cytokine Growth Factor Rev.*, **7**, 223–229 (1996).
14) Komori A., Yatsunami J., Suganuma M., Okabe S., Abe S., Sakai A., Sasaki K., Fujiki H., *Cancer Res.*, **53**, 1982–1985 (1993).
15) Komori A., Suganuma M., Okabe S., Zou X., Tius M. A., Fujiki H., *Cancer Res.*, **53**, 3462–3464 (1993).
16) Lee H., Herrmann A., Deng J. H., Kujawski M., Niu G., Li Z., Forman S., Jove R., Pardoll D. M., Yu H., *Cancer Cell*, **15**, 283–293 (2009).
17) Zou Z., Huang B., Wu X., Zhang H., Qi J., Bradner J., Nair S., Chen L. F., *Oncogene*, **33**, 2395–2404 (2014).
18) Hashimoto Y., *Bioorg. Med. Chem.*, **10**, 461–479 (2002).
19) Noguchi-Yachide T., Sakai T., Hashimoto Y., Yamaguchi T., *Bioorg. Med. Chem.*, **23**, 953–959 (2015).
20) Picaud S., Strocchia M., Terracciano S., Lauro G., Mendez J., Daniels D. L., Riccio R., Bifulco G., Bruno I., Filippakopoulos P., *J. Med. Chem.*, **58**, 2718–2736 (2015).
21) Zuber J., Shi J., Wang E., Rappaport A. R., Herrmann H., Sison E. A., Magoon D., Qi J., Blatt K., Wunderlich M., Taylor M. J., Johns C., Chicas A., Mulloy J. C., Kogan S. C., Brown P., Valent P., Bradner J. E., Lowe S. W., Vakoc C. R., *Nature* (London), **478**, 524–528 (2011).
22) Shibata Y., Sasaki K., Hashimoto Y., Iwasaki S., *Chem. Pharm. Bull.*, **44**, 156–162 (1996).
23) Miyachi H., Ogasawara A., Azuma A., Hashimoto Y., *Bioorg. Med. Chem.*, **5**, 2095–2102 (1997).
24) Noguchi T., Miyachi H., Katayama R., Naito M., Hashimoto Y., *Bioorg. Med. Chem. Lett.*, **15**, 3212–3215 (2005).
25) Kagechika H., Kawachi E., Hashimoto Y., Himi T., Shudo K., *J. Med. Chem.*, **31**, 2182–2192 (1988).
26) Nakajima O., Sugishita Y., Hashimoto Y., Iwasaki S., *Biol. Pharm. Bull.*, **17**, 742–744 (1994).